Special Interest Group Drug-Design
December 1st, 2020

VIRTUAL SCREENING USING APPROVED DRUGS: IN SILICO EVALUATION OF ANTI HAT POTENTIALS

Raíssa Santos de Lima[1], Manuela Leal da Silva[2]

[1] Oswaldo Cruz Institute/RJ, [2]University of Rio de Janeiro/ RJ

E-mail: raissa.lima@ioc.fiocruz.br

Introduction

Human African Trypanosomiasis (HAT), also called sleeping sickness, is a neglected disease caused by the parasite *Trypanosoma brucei*. The treatment of HAT has two main drugs, fexinidazole and melarsoprol, the first of which has serious side effects, such as psychosis and personality disorder. Melarsoprol is administered parenterally, which requires hospitalization, in addition to presenting post-treatment reactive encephalopathy (MAKHANI et al., 2019). The problem with HAT is that the drugs used in the treatment have several adverse effects (personality changes, psychosis and hyponatremia), negatively influencing therapeutic adherence. Due to the adverse effects and difficulty in administering the drugs, the treatment has low therapeutic adherence.

Objectives

The objective of the work is to find potential substances that can act by inhibiting the 24-c-sterol-methytranferase (SMT) protein, which participates in the ergosterol biosynthesis, an important metabolic pathway for the parasite.

Methods

Workflow of the methods employed:

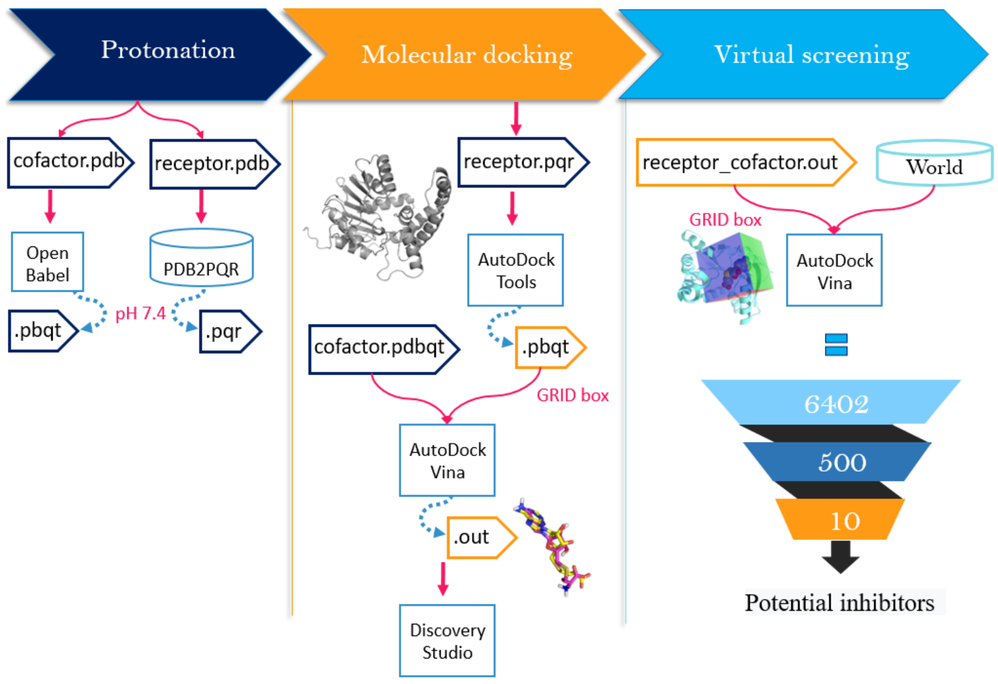

Figure 1: The methodology is in blue, the programs are circled in yellow.

Results

Model - Template

- 3BUS –*Lentzea aerocolonigenes* transferase;
- Model obtained from previous works; (WERNECK; GOMES; DA SILVA, 2017)
- SAM cofactor;

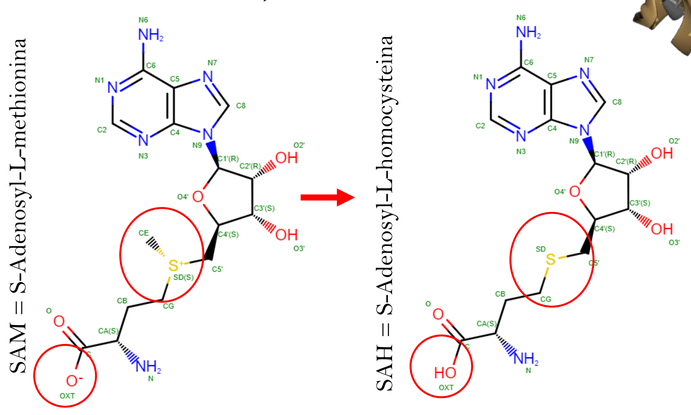

Figure 3: Chemical modification of the SAM cofactor to the SAH form.

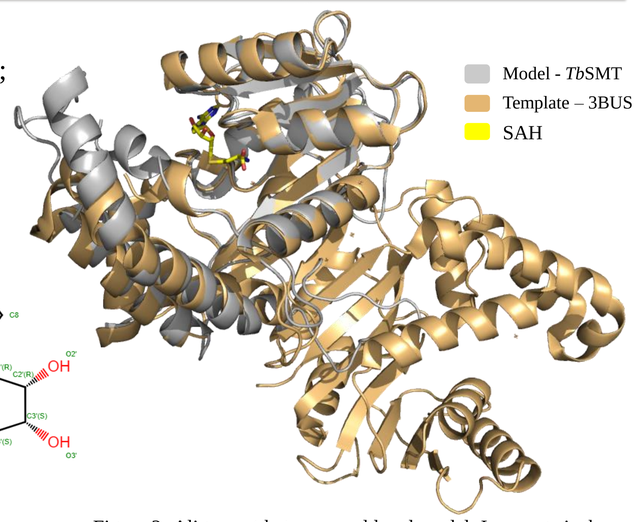

Figure 2: Alignment between mold and model. In orange is the 3BUS template with the complexed SAH cofactor (represented on yellow carbon sticks). In gray the model predicted for the *Tb*SMT protein.

Redocking 3BUS - SAH

- RMSD = 1.355 Å;
- Binding energy: -7,7 kcal/mol;

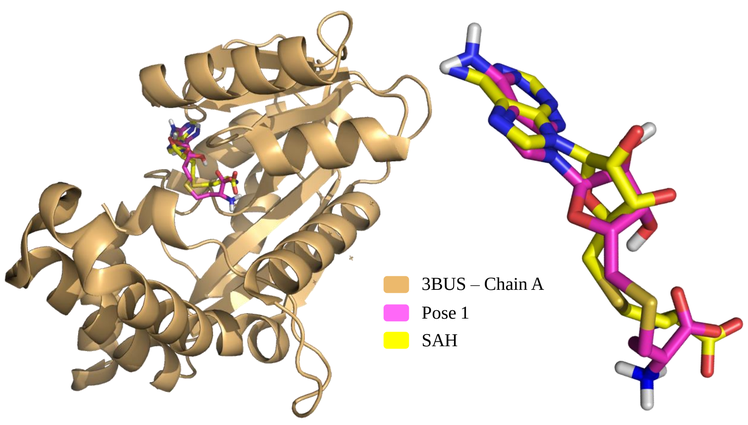

Figure 5: Result of the redocking of the SAH cofactor. In orange, the A chain of the 3BUS structure. Represented in sticks with carbons in yellow is the ligand SAH in its experimentally resolved form and with carbons in pink the result of redocking.

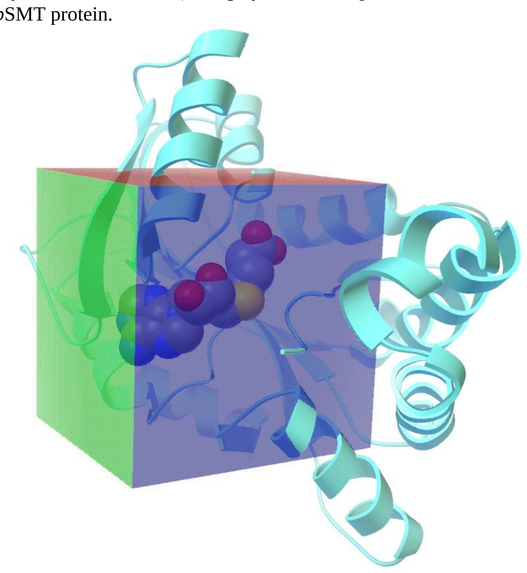

Figure 4: Grid Box formulated with the AutoDock Tools program (center x: 15.278; y: 28.139; z: 30.662; and size x: 60; y: 60; z: 54) . In cyan the protein *Tb*SMT and represented by spheres with gray carbons is the ligand SAH.

Docking

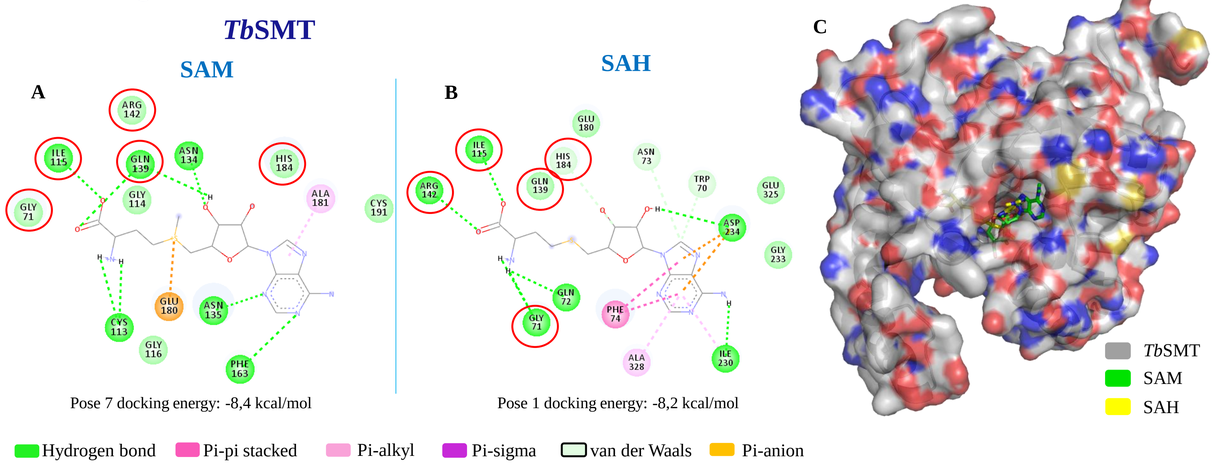

Figure 6: Result of the docking of the SAH and SAM cofactor. A – Discovery Studio graph of the interactions between the ligand SAM and *Tb*SMT. B – Discovery Studio graph of the interactions between the ligand SAH and *Tb*SMT. C - Represented by surface with carbons in gray is the TbSMT protein. Represented on sticks with yellow carbons is the result of the SAH ligand and with green carbons the result of the SAM ligand.

Virtual screening

*Tb*SMT

Table 1: Top ten results from VS with FDA using *Tb*SMT

DrugBank code	Binding energy (kcal/mol)	Mechanism of action
DBX22X	-13.9	Inhibition of RNA synthesis
DBX63X	-12.3	Produces cytotoxic species that will cause oxidative damage to the cancer cell
DBX69X	-11.3	Activation of 5-HT receptors located in intracranial blood vessels
DBX38X	-11.2	HCV NS3/4A protease inhibitor
DBX33X	-11.2	Interferes with DNA synthesis
DBX87X	-11.1	Dual AVP antagonist with affinity for vasopressin receptors
DBX21X	-11.1	Interacts as an agonist of the transmembrane domain of the human TPO receptor
DBX07X	-11.1	Binds to mitochondrial enzymes carnitine palmitoyltransferase
DBX59X	-11.1	Inhibits protein kinase C alpha (PKCalpha)
DBX61X	-11	Binding to antigen-associated lymphocyte integrin1 (LFA-1)

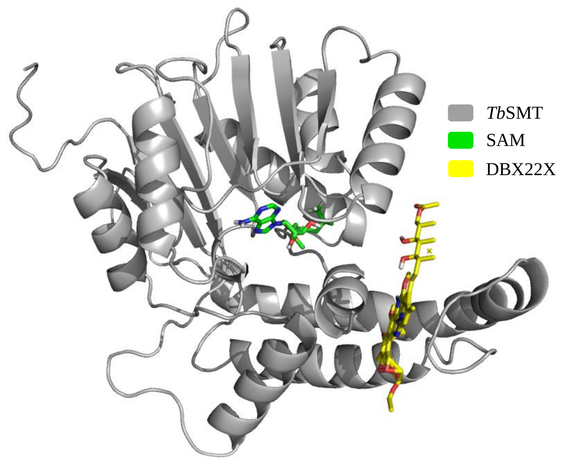

Figure 7: Docking result showing the best classified substance. In gray is the TbSMT enzyme. The green coffer is the SAM cofactor, the yellow substance DBX22X.

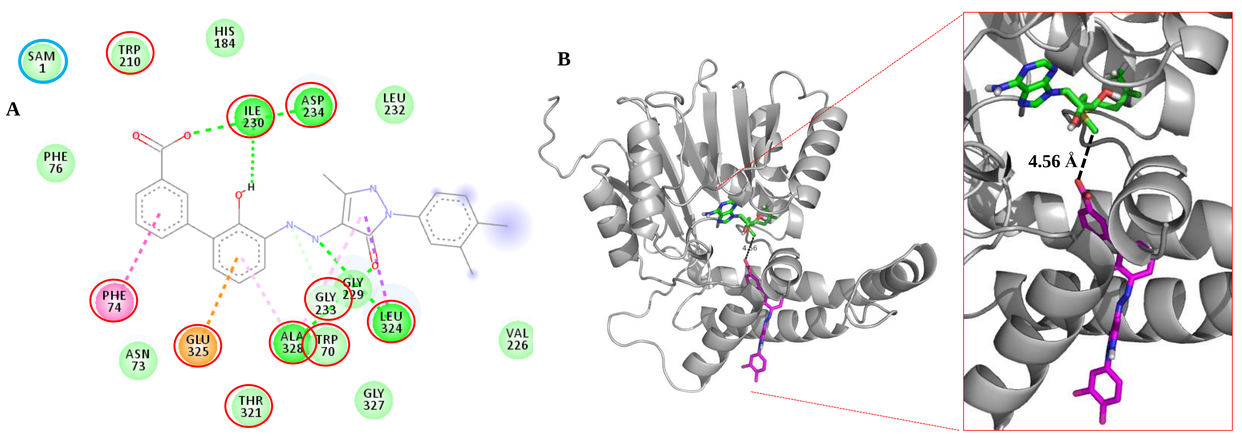

Figure 8: Analysis of interactions between DBX21X ligand and *Tb*SMT enzyme amino acids. In A is the graph of the types of chemical bonds made between the substance DBX21X and the target. Highlight circles for important amino acids. In B is the three-dimensional representation of the interaction and the measurement of the distance between the cofactor (green sticks) and the substance (magenta sticks).

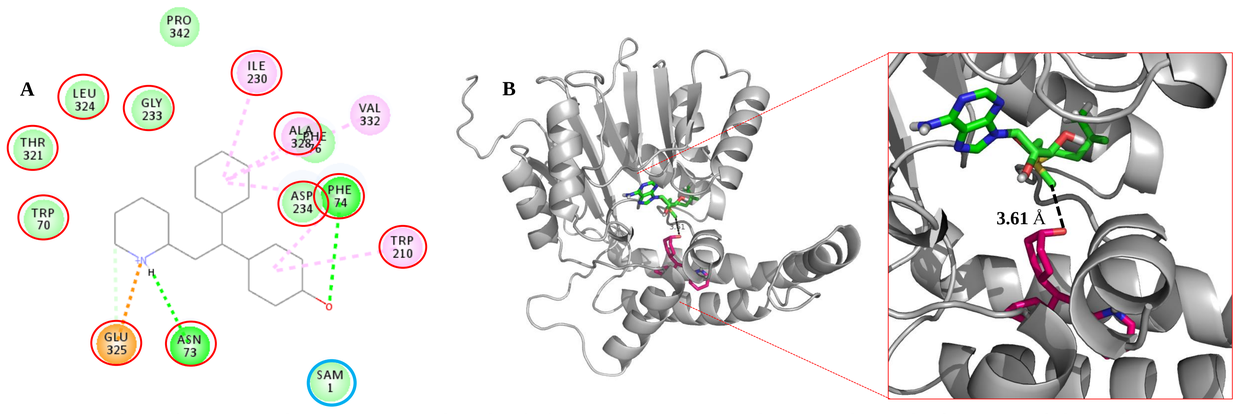

Figure 9: Analysis of interactions between DBX07X ligand and *Tb*SMT enzyme amino acids. In A is the graph of the types of chemical bonds made between the substance DBX07X and the target. Highlight circles for important amino acids. In B is the three-dimensional representation of the interaction and the measurement of the distance between the cofactor (green sticks) and the substance (pink sticks).

Conclusion and Perspectives

The *Tb*SMT model obtained based on PDBid: 3BUS (WERNECK; GOMES; DA SILVA, 2017) was used to search for potential inhibitors. First with the 3BUS, redocking with SAH was carried out and the parameters were validated. The docking was done with *Tb*SMT and SAH and then with the SAM form. With the discovery studio program, chemical interactions were seen and we concluded that the pose 7 of the SAM had more connections in common with the SAH form. With the cofactor attached, the VS of the World subset of ZINC15 was made, and the first 10 substances were analyzed. Highlight for two of these substances that interacted with the cofactor, having the potential to act in place of the natural substrate and preventing the reaction, inhibiting the enzyme. In the future, more analysis of interactions and in vitro tests will be carried out.

References

- MAKHANI, L. et al. **Tropical Diseases, Travel Medicine and Vaccines**, v. 5, n. 1, p. 1–12, 2019.
- THOMPSON, C. K.; GODFREY, S. S.; THOMPSON, R. C. A. **International Journal for Parasitology: Parasites and Wildlife**, v. 3, n. 2, p. 57–66, 2014.
- TROTT, O.; OLSON, A. NIH Public Access. **Journal of Computational Chemistry**, v. 31, n. 2, p. 455–461, 2010.
- VERLI, H. **Bioinformática da Biologia à Flexibilidade Molecular**. [s.l: s.n.]v. 53

Acknowledgment

FIOCRUZ
CAPES